

# Catheter-based intraluminal optical coherence tomography: comparison with digital light microscopy of ureter wall morphometry in porcine specimens

Ulrike L. Mueller-Lisse<sup>1,2</sup>, Margit Bauer<sup>4</sup>, Oliver A. Meissner<sup>3,5</sup>, Maximilian F. Reiser<sup>3</sup>, Christian G. Stief<sup>2</sup>, Ullrich G. Mueller-Lisse<sup>3\*</sup>

<sup>1</sup>Interdisciplinary Oncology Center - IOZ Muenchen, <sup>2</sup>Departments of Urology and <sup>3</sup>Radiology, University of Munich, and Department of Surgery, <sup>4</sup>Technical University of Munich, and <sup>5</sup>Steinbeis University, Berlin, Germany

\*Corresponding author: Ulrike L. Mueller-Lisse, Email: muellerlisse@gmx.de or ullrich.mueller-lisse@med.uni-muenchen.de

Competing interests: The authors have declared that no competing interests exist.

Abbreviations used: OCT, optical coherence tomography; DLM, digital light microscopy; H&E, hematoxylin and eosin; NIR, near infrared; O1, observer 1; O2, observer 2

Received March 8, 2015; Revision received April 19, 2015; Accepted June 3, 2015; Published June 10, 2015

## ABSTRACT

**OBJECTIVE:** Reproducibility and agreement of width estimates for urothelium, lamina propria, and muscle layer of normal porcine ureter wall *ex vivo* were compared between catheter-mounted, intraluminal cross-sectional optical coherence tomography (OCT), as a new destruction-free optical imaging method that could be applied clinically to examine the upper urinary tract from within if found to reliably delineate its different anatomical layers, and whole-mount low-power digital light microscopy (DLM).

**MATERIALS AND METHODS:** Eleven *ex-vivo*-specimens of porcine ureter were flushed with normal saline solution prior to OCT (catheter diameter, 0.014 inch, wavelength,  $1300 \pm 20$  nm, LightLab Imaging, Inc., Westford, MA, USA) at marked locations. Ring-shaped (3 mm) ureter specimens were fixed in 4%-formalin, cut, whole-mounted, and hematoxylin-eosin-stained. Respective thicknesses of urothelium, lamina propria, and muscle layer of the ureter wall were compared between OCT and matching DLM slides (Axioplan2, Carl-Zeiss-Corporation, Jena, Germany) by two independent observers, applying Bland-Altman plots and paired-data-Student-T-testing at  $P < 0.05$ .

**RESULTS:** Width estimates were reproducibly higher for urothelium by a factor of about 1.4 at OCT ( $60 \pm 9$ – $96 \pm 18$   $\mu\text{m}$ ) compared to DLM ( $45 \pm 12$ – $68 \pm 9$   $\mu\text{m}$ ,  $P < 0.01$ ), similar for lamina propria (OCT,  $191 \pm 21$ – $233 \pm 44$   $\mu\text{m}$ ; DLM,  $189 \pm 48$ – $326 \pm 58$   $\mu\text{m}$ ), and variable for muscle layer (OCT,  $355 \pm 109$ – $631 \pm 42$   $\mu\text{m}$ ; DLM,  $454 \pm 97$ – $527 \pm 121$   $\mu\text{m}$ ).

**CONCLUSIONS:** It appears that OCT reliably delineates ureter wall layers demonstrated by DLM, and that intra-observer reproducibility of the width of urothelium and lamina propria is high for both OCT and DLM, width estimates of lamina propria are reliable at OCT, and width of urothelium is reproducibly overestimated at OCT when compared with DLM.

**Keywords:** digital light microscopy, morphometry, optical coherence tomography, urinary tract, ureter

## INTRODUCTION

Optical coherence tomography (OCT) applies coherent near infra-red light (NIR, wavelength range, 800–1400 nm) to obtain cross-sectional images of biological tissues. Based on the principle of a Michelson interferometer, interference of coherent NIR light is used to determine depth of reflection from different tissue layers [1,2]. Biological tissues other than the vitreous body of the eye, such as human skin or vessel walls, strongly scatter NIR light but allow for OCT measurements with a sub-surface depth of up to 2 mm [1,3,4]. Catheter-based OCT devices have been developed to study blood vessels and hollow organs from

inside their lumen in real time, with a spatial resolution of less than 20  $\mu\text{m}$  [2-6]. In urology, OCT applications focus on the urinary bladder. Normal urothelium shows with multiple layers, while tissue edema and loss of distinct layering is associated with pathologic conditions [7-9]. OCT may help to guide bladder biopsies [10]. In the upper urinary tract, extracorporeal OCT has demonstrated differentiation of tissue microstructure post mortem [1], while intraluminal OCT of porcine upper ureters *ex vivo* distinguishes between urothelium, lamina propria, and muscle layer [2]. Intraluminal OCT could potentially be useful in both urological endoscopy, to obtain estimates of the depth of tissue invasion of particular lesions, and gross surgical pathology, to locate

and measure lesions within the upper urinary tract and target histopathological analysis. Ideally, if OCT were to be applied as an approach to an almost microscopic depiction of normal and pathological tissue *in vivo* and in gross pathology specimens, OCT should compare with light microscopy not only in the distinction of different tissue layers, but also in similar estimates of their respective morphometric dimensions. Thus, as an indicator of the reliability of OCT morphometry, we compared width estimates for urothelium, lamina propria, and muscle layer of normal porcine ureter wall *ex vivo* and their respective reproducibility by different observers between catheter-mounted intraluminal OCT, with a transversal spatial resolution of 15  $\mu\text{m}$ , and low-power digital light microscopy (DLM), with a spatial resolution of 4  $\mu\text{m}$ .

## MATERIALS AND METHODS

### Preparation of porcine upper ureter specimens

Eleven porcine kidneys with adherent upper ureters were obtained fresh from the municipal slaughterhouse, transported to the laboratory in air-tight containers at ambient pressure and temperature, and thoroughly rinsed, inside and out, with normal saline solution, within two hours of slaughtering. Adherent tissues were removed to expose the renal hilus and upper ureter of each specimen. Specimens were then fixed to a Styrofoam pad, such that the long axis of the ureter was orthogonal to the long axis of the kidney. The Styrofoam pad was placed in a shallow plastic tub that allowed easy horizontal access to the kidney and ureter. The distal cut edge of the ureter was identified, and the tip of a 7F catheter sheath with a dilator and a side port for flush lines (Schleusen-Set 7F, Peter Pflugbeil GmbH Medizinische Instrumente, Zorneding, Germany) was inserted after flushing with normal saline solution. A size-1 (4 Ph. Eur.) surgical suture (Ethicon Ethibond Excel, Johnson & Johnson Intl.) was tied around the ureter, approximately 3 mm proximal to the cut edge, to secure the position of the catheter sheath. The dilator was removed, and a 10-ml syringe (Terumo Syringe, Terumo Europe N.V., Leuven, Belgium) with normal saline solution was connected to the side port of the catheter sheath via a three-way stop cock (Discifix-3, B. Braun Melsungen AG, Melsungen, Germany), with the third way opening to surrounding air to allow for draining. For OCT measurements, the urinary collecting system was filled with normal saline solution, such that the cross-sectional diameter of the proximal ureter was 3–4 mm and the folds of the ureter were still being seen on the OCT images.

### Optical coherence tomography (OCT)

OCT measurements were performed with a catheter-mounted prototype system for intraluminal examinations (M1, LightLab Imaging, Inc., Westford, MA, USA). The OCT system includes a source for coherent NIR light (wavelength,  $1300 \pm 20$  nm), and a beam splitter that directs half of the light into the measurement arm and half into the reference arm of a Michelson-type interferometer. The measurement arm features an electric drive that rotates the OCT optical fiber (diameter, 400  $\mu\text{m}$ ), whose distal end includes a miniature mirror that emits and receives NIR light, inside a catheter probe of 2.4 m in length. Integrity of the fiber and position of the mirror is checked by a visible pilot light. The OCT catheter was inserted into the porcine upper ureter through the catheter

sheath. The location for the pilot light of the OCT probe was marked on the outside of each porcine ureter by one dot of a permanent ink marker pen with a felt tip. The permanent ink had previously been tested in our laboratory on tissue removed from the distal cut edge of porcine ureter specimens during preparation for previous experiments to be resistant against 4% formalin solution for at least one week. Immediately after one another, two OCT examinations, (A) and (B), were performed of each specimen, including complete removal and new insertion of the OCT probe into the respective ureter. At each OCT examination, a two-dimensional, cross-sectional OCT image of the porcine ureter was acquired, at the location previously marked.

OCT images were displayed on the system monitor, either as grey-scale images or in shades of sepia, both during OCT measurements and after retrieval of data previously archived in compression-free .tiff format. According to manufacturer's information (LightLab Imaging, Inc., Westford, MA, USA), spatial resolution of cross-sectional OCT images is approximately 15  $\mu\text{m}$  in the axial plane, and 25  $\mu\text{m}$  through-plane. Two independent observers (O1, O2) performed at least three measurements each of the width of urothelium, lamina propria, and muscle layer in different quadrants (i.e., right and left upper and lower quadrants, respectively) of each cross-sectional OCT image, respectively, applying linear distance measurement functions of the OCT system. Since there were 11 different specimens, each OCT width estimate was based on at least 33 different distance measurements. Each observer repeated those width estimates once for each OCT examination, such that there were four sets of distance measurements (D1 through D4) per observer for each specimen.

### Digital light microscopy (DLM)

Subsequently, porcine upper ureters were cut transversely at locations previously marked, to obtain ring-shaped cross-sections of approximately 3 mm in width. Ureter sections were individually transferred to vials containing 4% formalin solution. After at least 24 hours of submersion, ureter sections were prepared for digital light microscopy (DLM), including embedding in paraffin blocks, cutting by means of a microtome, and staining with hematoxylin-eosin (H&E) stain. For each ureter section, two different DLM slides were obtained. DLM (Axio-plan2, with AxioVs40V4.2.0.0 software and Plan Neofluar 5x/0.15 lens system, Carl Zeiss Corporation, Jena, Germany) was performed at low power, with a spatial resolution of approximately 4  $\mu\text{m}$ . DLM images (AxioCam HRc, Carl Zeiss Corporation, Jena, Germany) were stored in compression-free .jpeg format. Applying image post-processing software of the DLM system, the two independent observers each performed 10 distance measurements to estimate the width of urothelium, lamina propria, and muscle layer in each DLM slide, respectively.

### Statistical evaluation

Applying spreadsheet calculation functions in Microsoft Excel 2003 (Microsoft Corporation), mean values, standard deviations, and differences were calculated for respective width estimates of urothelium, lamina propria, and muscle layer at OCT and DLM, for Bland-Altman plots [11] and Student's-T-test for paired data with two tails [12], on a significance level of  $P < 0.05$ .

## RESULTS

Cross-sectional intra-luminal OCT images and DLM slides were obtained in 11 different specimens of porcine upper ureters. Display of the cross-sectional OCT images on the monitor of the OCT system demonstrated the innermost layer, deemed to represent urothelium,

with intermediate brightness, the second layer, assumed to represent lamina propria, with high brightness, and the third layer, considered to represent the muscle layer, with low brightness (Fig. 1 and Fig. 2).

In some specimens, the ureter folds appeared more rounded at OCT than at DLM (Fig. 1), while they were similarly rounded in other specimens (Fig. 2).

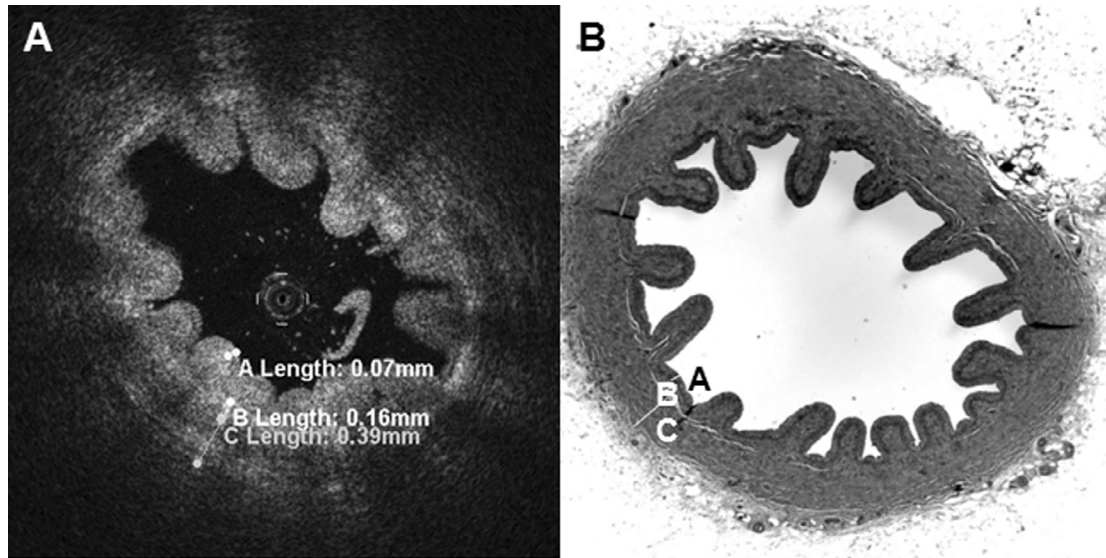


Figure 1. Comparison of optical coherence tomography (OCT, panel A, in shades of grey) and low-power digital light microscopy (DLM, panel B, after hematoxylin-eosin-staining, in shades of grey) demonstrates markers of respective width of urothelium (length A), lamina propria (length B) and muscle layer (length C).

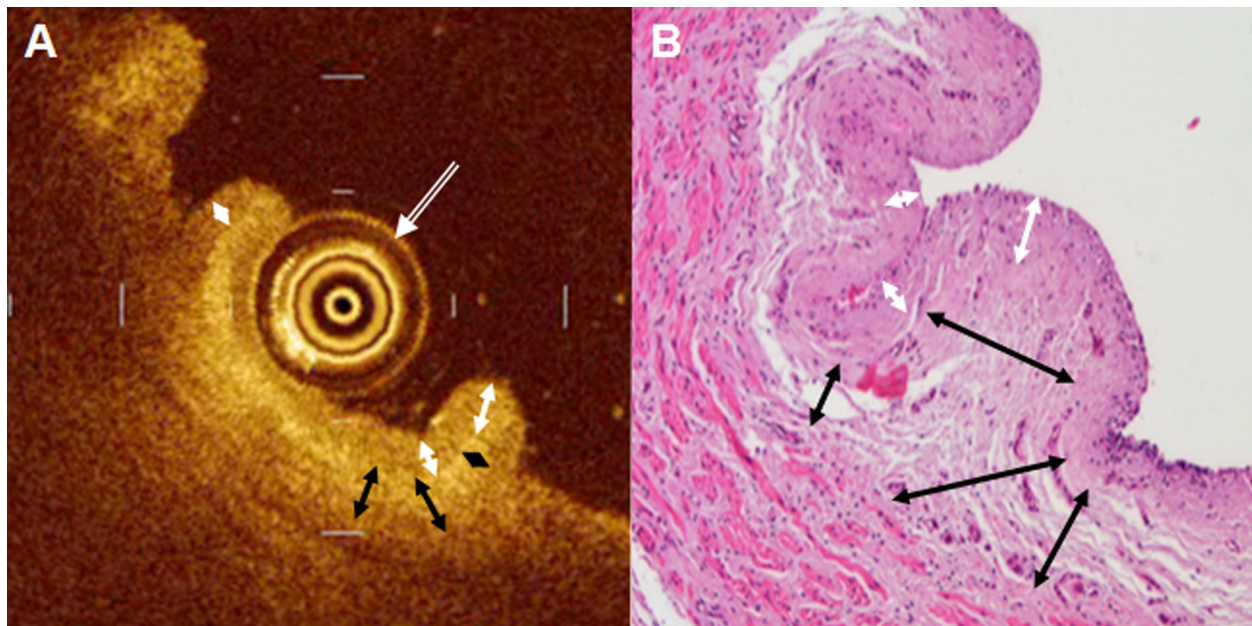
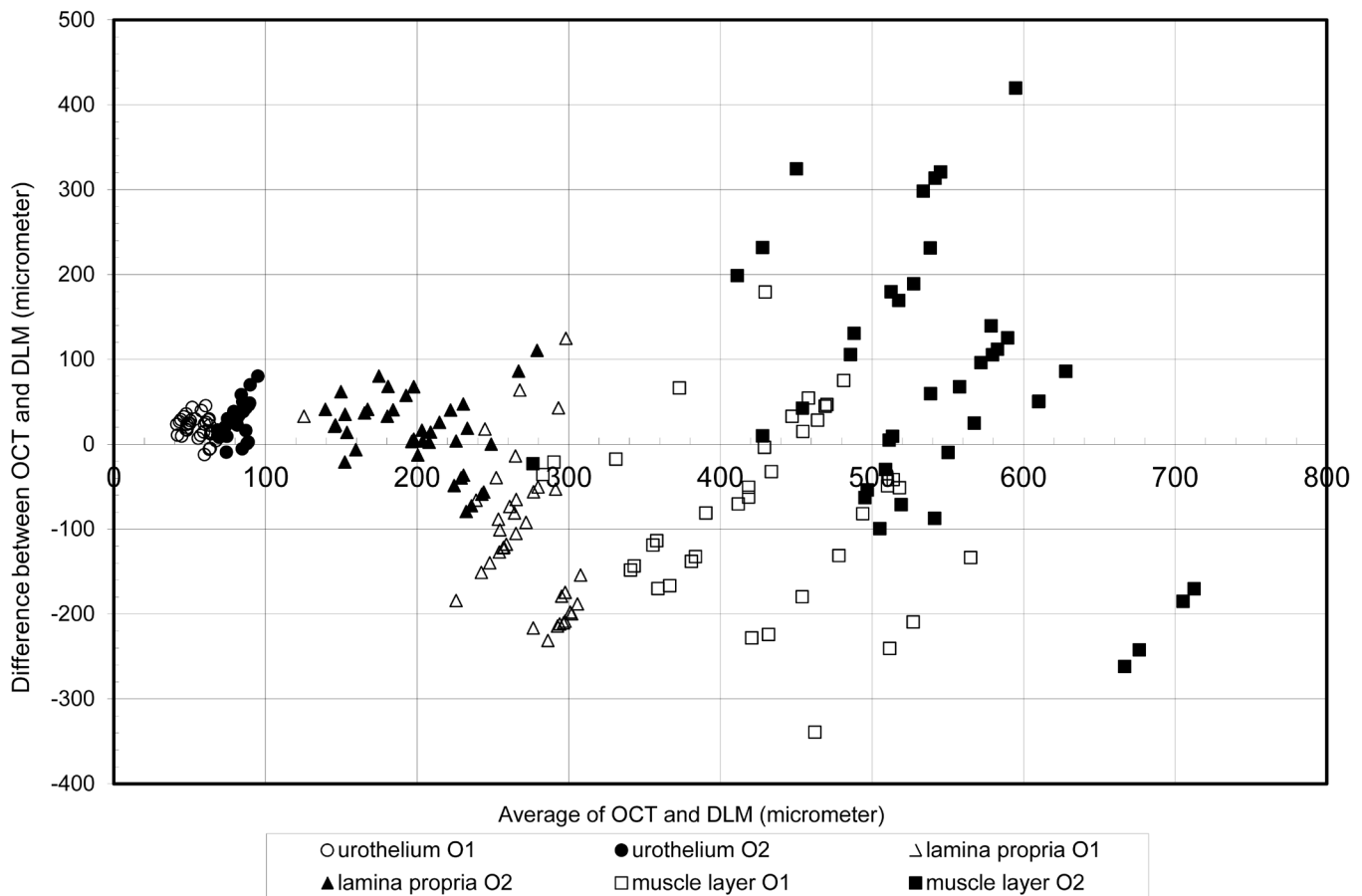


Figure 2. Detail views of optical coherence tomography (OCT, in shades of sepia), with an in-plane resolution of approximately 15  $\mu\text{m}$  (A), and corresponding low-power digital light microscopy (DLM, after hematoxylin-eosin staining), with an in-plane resolution of approximately 4  $\mu\text{m}$  (B) of a normal porcine upper ureter wall specimen *ex vivo*. Two-pointed white arrows demarcate perceived width of urothelium, two-pointed black arrows demarcate perceived width of lamina propria in A and B. Double-lined white arrow in A marks the intraluminal OCT probe.

Respective width estimates of the urothelium were significantly higher in OCT images than in DLM slides, by a factor of about 1.4, for both observers and all measurements. However, O1 repetitively measured urothelial width smaller than did O2 on both OCT images (by about two image points) and DLM slides (by about four image points).

Reproducibility of mean width was within 10% or about one-half image point of the average of the means at OCT, with standard deviations of about one image point, and within 2.5% or about one-half image point at DLM, with standard deviations of about two image points, for both observers, (**Fig. 3, Table 1**).



**Figure 3.** Bland-Altman plot for corresponding width estimates of urothelium, lamina propria, and muscle layer of porcine upper ureter *ex vivo*, based on OCT images (OCT) and low-power digital light microscopy (DLM) for two independent observers (O1, O2).

For all measurements, respective width estimates of the lamina propria were significantly smaller in OCT images than in DLM slides for O1, while there were no significant differences for O2. However, while inter-observer results for the lamina propria were similar at OCT, O1 repetitively estimated width of the lamina propria larger than did O2 at DLM. Reproducibility of mean width was within 7% or about one image point (O1) and 11% or about one-and-one-half image points (O2) of the average of the means at OCT, with standard deviations of about three image points, and within 3.2% or about two image points (O1) and 2.6% or about one image point (O2) at DLM, with standard deviations of about 12–20 image points, respectively. Depending on individual mean values, width estimates of the lamina propria exceeded width estimates of the urothelium by factors between 2 and 4 (**Fig. 3, Table 1**).

Respective width estimates of the muscle layer tended to be smaller at OCT when compared with DLM for O1, while there were no significant differences for O2. However, O1 repetitively measured width of the muscle layer smaller than did O2, both on OCT images and on DLM slides. Reproducibility of mean width was within 12.5% or about three image points (O1) and 15.5% or about six image points (O2) of the average of the means at OCT, with standard deviations of about three to seven image points, and within 2% or about two image points (O1) and 5% or about five image points (O2) at DLM, with standard deviations of about 22–35 image points, respectively (**Fig. 3, Table 1**).

Ranges of overall width of the three layers of the ureter wall, as the respective sums of the mean values of lines D1(A) to D4(B) in **Table 1**, were 620–724  $\mu\text{m}$  for O1 and 791–942  $\mu\text{m}$  for O2 at OCT, and 807–842  $\mu\text{m}$  for O1 and 742–792  $\mu\text{m}$  for O2 at DLM.

**Table 1. Repetitive measurements of width of urothelium, lamina propria, and muscle layer by means of optical coherence tomography (OCT) and digital light microscopy (DLM) in specimens of porcine upper ureter *ex vivo* (n = 11).**

	Urothelium (µm)		Lamina propria (µm)		Muscle layer (µm)	
	OCT <sup>a</sup>	DLM <sup>a</sup>	OCT <sup>b</sup>	DLM <sup>b</sup>	OCT <sup>c</sup>	DLM <sup>c</sup>
Results for observer No. 1 (mean width in µm ± standard deviation)						
D1(A)	63 ± 16	47 ± 14	202 ± 59	306 ± 88	355 ± 109	454 ± 97
D2(A)	64 ± 12	45 ± 12	209 ± 32	326 ± 58	450 ± 71	471 ± 86
D3(B)	68 ± 9	47 ± 14	214 ± 52	306 ± 88	363 ± 84	454 ± 97
D4(B)	60 ± 9	45 ± 12	228 ± 55	326 ± 58	436 ± 69	471 ± 86
Results for observer No. 2 (mean width in µm ± standard deviation)						
	OCT <sup>d</sup>	DLM <sup>d</sup>	OCT <sup>e</sup>	DLM <sup>e</sup>	OCT <sup>f</sup>	DLM <sup>f</sup>
D1(A)	95 ± 10	68 ± 9	191 ± 21	189 ± 48	579 ± 96	485 ± 142
D2(A)	93 ± 13	66 ± 9	208 ± 23	199 ± 46	631 ± 42	527 ± 121
D3(B)	93 ± 18	68 ± 9	208 ± 49	189 ± 48	490 ± 104	485 ± 142
D4(B)	96 ± 18	66 ± 9	233 ± 44	199 ± 46	613 ± 45	527 ± 121

<sup>a</sup> $P < 0.0005$  to  $P < 0.005$ ; <sup>b</sup> $P < 0.005$  to  $P < 0.05$ ; <sup>c</sup> $P < 0.01$  to  $P > 0.5$ ; <sup>d</sup> $P < 0.0005$  to  $P < 0.01$ ; <sup>e</sup> $P > 0.07$  to  $P > 0.5$ ; <sup>f</sup> $P > 0.05$  to  $P > 0.5$

D1, D2, D3, D4, distance measurements 1 to 4 to determine respective width of different wall layers of porcine ureter; (A), (B), different OCT examinations of same specimens of porcine ureters *ex vivo*; distance measurements were repeated once for DLM.

## DISCUSSION

The most important findings of our study of the porcine ureter were that intra-observer reproducibility of the width of the urothelium and the lamina propria was high for both OCT and DLM, that width estimates of the lamina propria were reproducibly similar between observers at OCT, and that width of the urothelium was reproducibly overestimated by a factor of about 1.4 at OCT when compared with DLM.

It has previously been shown by histological analysis at light microscopy that the porcine upper urinary tract closely resembles the human upper urinary tract in its morphological structure [13]. Urothelium and lamina propria of the porcine ureter *ex vivo* are reliably delineated at light microscopy [13] and at OCT, with substantial inter-observer agreement [2]. Light microscopy, particularly with H&E staining, is the accepted standard of histological analysis in clinical practice. Light microscopy therefore appeared to be the most suitable reference standard for our observations in OCT images, although its observations are based on *ex-vivo* tissues whose morphometric properties may be altered by dehydration during the preparation of histology slides, particularly during the process steps of fixation, embedding, and mounting [14].

In our study, both DLM and OCT reproducibly demonstrated three distinct tissue layers of the ureter. At DLM, those three layers were identified as urothelium, lamina propria, and muscle layer, while a fourth layer, the adventitia [15], was not regularly seen. The adventitia may have been removed during preparation of our specimens for OCT, because it has been described to blend with both the renal capsule and the surrounding connective tissue of the posterior abdominal wall [15]. Light microscopy identifies the thin basal lamina as the true borderline between the urothelium, which typically consists of four to five layers of transitional epithelial cells, from the lamina propria, which mainly consists of dense fibroconnective tissue, mostly elastic fibers, and scarce lymphatic or blood vessels [15]. The most likely explanation

for the border perceived at OCT between the first and the second layer of the ureter wall, deemed to represent the urothelium and the lamina propria, respectively, appears to be the increase in scatter or reflection of NIR light at the surfaces of the elastic fibers of the lamina propria. Based on this assumption, the borderline would not be defined by the basal lamina, which in itself is below the spatial resolution of the OCT system applied here, but by the transition of the cellular urothelium to the surface of the fibroconnective tissues immediately underneath. It remains unclear at this juncture if that transition at OCT is a valid surrogate marker for the basal membrane in a clinical sense, i.e., as a marker of intactness of the basal membrane in a disease process. Since both the mean and the variation in width estimates of the urothelium demonstrated similarly high intra-observer reproducibility at OCT and DLM, it appears that the transition from urothelium to lamina propria is well perceived by both modalities, and that the reproducible variation in measurements reflects differences in width that are mostly due to ureter wall folding, which was apparent at both OCT and DLM, although with variable appearance.

However, for width estimates of the urothelium at OCT and DLM, intra-observer reproducibility was far better than inter-observer reproducibility. Since width estimates for the lamina propria were highly reproducible at OCT, it appears unlikely that the border between urothelium and lamina propria was perceived differently. Rather, with a reproducible inter-observer difference of 1–2 image points at OCT, it appears likely that systematic differences in measurement technique between observers were accountable.

Independent of the observers, width of the urothelium was reproducibly overestimated by a factor of about 1.4 at OCT when compared with DLM. While we failed to find estimates of tissue shrinkage through preparation for light microscopy of urinary tract specimens, it has previously been shown for quantitative histological analysis of atherosclerotic coronary artery specimens post mortem that they exhibit

several artificial dimension changes during processing, which lead to disproportionate results when comparing lumen and vessel dimensions [16]. Therefore, differences in width estimates of normal urothelium between OCT and DLM may be due to tissue shrinkage associated with the preparation of DLM slides. In turn, tissue shrinkage may be less pronounced or absent in the lamina propria, with its high content of fibroconnective tissue.

Substantial intra- and inter-observer reproducibility of the width of the ureteral lamina propria at OCT suggests that OCT reliably depicts the dense fibroconnective tissues of the inner layer of the lamina propria. However, light microscopy-based histology of the ureter demonstrates an outer layer of the lamina propria, with lower density of fibroconnective tissues, that has been regarded by some as a submucosal layer of the ureter wall [15]. That outer layer appears to merge with the muscle layer, with no definitive borderline between the two. It appears likely that the decrease in density of fibroconnective tissue changes optical properties of the tissue, such that a border could be perceived at OCT that does not appear to exist at DLM. This would explain the differences in inter-observer reproducibility of the mean width of the lamina propria in our study, which was high for OCT and low for DLM. If at DLM observer 1 had considered the “submucosal” layer to be part of the lamina propria, while observer 2 had regarded it to be part of the muscle layer, the inter-observer variation in mean width of lamina propria and muscle layer would be explained.

Width estimates for the muscle layer varied the widest, both within and between OCT, DLM, and the two independent observers. At intraluminal OCT of the upper urinary tract, NIR light reaching the muscle layer is subject to both increasing scatter and decreasing tissue penetration, due to increasing distance from the light source. While this would explain decreased reliability of OCT in deeper tissue layers, it could not account for similar observations at DLM. In addition, overall width of the ureter wall was estimated to be smaller than 1 mm both at OCT and DLM in this study. Since it has been demonstrated that OCT with NIR light penetrates biological tissue to a depth of 2 mm [1], the wall of the normal porcine ureter should be completely within reach of intraluminal OCT. Thus, it appears more likely that the outer boundaries of the muscle layer are generally either difficult to define or demonstrate biological variability, which would affect both OCT and DLM similarly.

Potential clinical applications of morphometric intraluminal OCT would include both urological endoscopy, to obtain estimates of the depth of tissue invasion by particular lesions, and gross surgical pathology, to locate and measure lesions within the upper urinary tract and target histopathological analysis. In both instances, knowledge of the normal width of the different ureter wall layers and of the respective proportion of the entire width of the ureter wall that each distinct layer requires could help to detect and locate pathologic tissue alteration.

## CONCLUSIONS

Our study of catheter-mounted OCT and DLM of normal porcine ureters *ex vivo* implies that both modalities reproducibly delineate the urothelium, lamina propria, and muscle layer of the porcine ureter wall *ex vivo*, that intra-observer reproducibility of the width of the urothelium and the lamina propria is high for both OCT and DLM, that width estimates of the lamina propria are reliable even between different observers

at OCT, and that width of the urothelium is reproducibly overestimated by a factor of about 1.4 at OCT when compared with DLM. Further research should be directed at the biological tissue properties that govern the perception of tissue borders in OCT examinations.

## Acknowledgements

The authors thank staff from LightLab, Inc., Westford, MA, USA, and Miss Monika Jaeger for technical assistance in obtaining and archiving OCT images acquired for the purposes of this study, and Gregor Babaryka, M.D., of the Department of Pathology of the University of University of Munich, for technical support with digital light microscopy and microphotography.

## References

1. Tearney GJ, Brezinski ME, Southern JF, Bouma BE, Boppart SA, et al. (1997) Optical biopsy in human urologic tissue using optical coherence tomography. *J Urol* 157: 1915-1919. PMID: [9112562](#)
2. Mueller-Lisse UL, Meissner OA, Babaryka G, Bauer M, Eibel R, et al. (2006) Catheter-related intraluminal optical coherence tomography (OCT) of the ureter: *ex-vivo* correlation with histology in porcine specimens. *Eur Radiol* 16: 2259-2264. doi: [10.1007/s00330-006-0191-8](#). PMID: [16572332](#)
3. Brezinski ME, Tearney GJ, Weissman NJ, Boppart SA, Bouma BE, et al. (1997) Assessing atherosclerotic plaque morphology: comparison of optical coherence tomography and high frequency intravascular ultrasound. *Heart* 77: 397-403. PMID: [9196405](#)
4. Fujimoto JG, Boppart SA, Tearney GJ, Bouma BE, Pitris C, et al. (1999) High resolution *in vivo* intra-arterial imaging with optical coherence tomography. *Heart* 82: 128-133. PMID: [10409522](#)
5. Tearney GJ, Brezinski ME, Southern JF, Bouma BE, Boppart SA, et al. (1997) Optical biopsy in human gastrointestinal tissue using optical coherence tomography. *Am J Gastroenterol* 92: 1777-1779. PMID: [9382040](#)
6. Meissner OA, Rieber J, Babaryka G, Oswald M, Reim S, et al. (2006) Intravascular optical coherence tomography: comparison with histopathology in atherosclerotic peripheral artery specimens. *J Vasc Interv Radiol* 17: 343-349. doi: [10.1097/01.RVI.0000195324.52104.00](#). PMID: [16517781](#)
7. Boppart SA, Bouma BE, Pitris C, Tearney GJ, Southern JF, et al. (1998) Intraoperative assessment of microsurgery with three-dimensional optical coherence tomography. *Radiology* 208: 81-86. doi: [10.1148/radiology.208.1.9646796](#). PMID: [9646796](#)
8. Jesser CA, Boppart SA, Pitris C, Stamper DL, Nielsen GP, et al. (1999) High resolution imaging of transitional cell carcinoma with optical coherence tomography: feasibility for the evaluation of bladder pathology. *Br J Radiol* 72: 1170-1176. doi: [10.1259/bjr.72.864.10703474](#). PMID: [10703474](#)
9. Zagaynova EV, Streltsova OS, Gladkova ND, Snopova LB, Gelikonov GV, et al. (2002) *In vivo* optical coherence tomography feasibility for bladder disease. *J Urol* 167: 1492-1496. PMID: [11832776](#)
10. Pan YT, Xie TQ, Cw, Du, Bastacky S, Meyer S (2003) Zeidel ML (2003) Enhancing early bladder cancer detection with fluorescence-guided endoscopic optical coherence tomography. *Opt Lett* 28: 2485-2487. PMID: [14690122](#)
11. Glantz SA (1997) Comparing two different measurements of the same thing: the Bland-Altman method. In: Glantz SA. *Primer of Biostatistics*. Fourth Edition. Chapter 8: How to test for trends. New York, St. Louis, San Francisco, Auckland, Bogota, Caracas, Lisbon, London, Madrid, Mexico City, Milan, Montreal, New Delhi, San Juan, Sydney, Tokyo, Toronto: McGraw-Hill Health Professions Division. pp 266-271.
12. Glantz SA (1997) Experiments when subjects are observed before and after a single treatment: the paired t test. In: Glantz SA. *Primer of Biostatistics*. Fourth Edition. Chapter 9: Experiments when each subject receives more than one treatment. New York, St. Louis, San Francisco, Auckland, Bogota, Caracas, Lisbon, London, Madrid, Mexico City, Milan, Montreal, New Delhi, San Juan, Sydney, Tokyo, Toronto: McGraw-Hill Health Professions Division. pp 283-291.
13. Desgrandchamps F, Moulinier F, Cochand-Priollet B, Wassef M, Teillac P, et al. (1997) Microscopic study of the pig ureteral urothelium. *J Urol* 157: 1926-1927. PMID: [9112564](#)

14. Leeson CR, Leeson TS, Paparo AA (1985) The preparation of tissues. In: Leeson CR, Leeson TS, Paparo AA. Textbook of Histology. Introduction. Philadelphia, London, Toronto, Mexico City, Rio de Janeiro, Sydney, Tokyo: WB Saunders Company. pp 5-10.
15. Leeson CR, Leeson TS, Paparo AA (1985) Excretory Passages. In: Leeson CR, Leeson TS, Paparo AA. Textbook of Histology. Part II. Histology of the organ systems. Chapter 13. The urinary system. Philadelphia, London, Toronto, Mexico City, Rio de Janeiro, Sydney, Tokyo: WB Saunders Company. pp 432-434.
16. Siegel RJ, Swan K, Edwalds G, Fishbein MC (1985) Limitations of postmortem assessment of human coronary artery size and luminal narrowing: differential effects of tissue fixation and processing on vessels with different degrees of atherosclerosis. *J Am Coll Cardiol* 5: 342-346. PMID: [3881498](https://pubmed.ncbi.nlm.nih.gov/3881498/)



This work is licensed under a Creative Commons Attribution-Non-Commercial-ShareAlike 4.0 International License: <http://creativecommons.org/licenses/by-nc-sa/4.0>